Ag Electrodeposited on Cu Open-Cell Foams for the Selective Electroreduction of 5-Hydroxymethylfurfural

Ag electrodeposited on Cu open-cell foams for the selective electroreduction of 5-hydroxymethylfurfural

Giancosimo Sanghez de Luna, Phuoc Hoang Ho, Alice Lolli, Francesca Ospitali, Stefania Albonetti, Giuseppe Fornasari, and Patricia Benito*

G. Sanghez de Luna, Dr. P. H. Ho, Dr. A. Lolli, Dr. F. Ospitali, Prof. S. Albonetti, Prof. G. Fornasari, Prof. P. Benito
Dip. di Chimica Industriale "Toso Montanari"
University of Bologna
Viale Risorgimento 4, 40136 Bologna (BO), Italy
E-mail: patricia.benito3@unibo.it

Supporting information for this article is given via a link at the end of the document.((Please delete this text if not appropriate))

Abstract: The electrocatalytic conversion of 5-hydroxymethylfurfural (HMF), a biomass platform molecule, to 2,5-bis(hydroxymethyl)furan (BHMF), a polymer precursor, is a fully sustainable route that operates at room temperature and pressure, using water as source of hydrogen, and avoids high H_2 pressures. In this work, we investigate the use of 3D electrocatalysts, made by Ag^0 electrodeposited on Cu open-cell foams (Ag/Cu), to improve the efficiency in the electrochemical conversion of HMF to BHMF in basic media at different HMF concentrations. For comparison purposes, Ag and Cu bulk foams as well as Ag, Cu and Ag/Cu foil counterparts are investigated. For diluted 0.02 M HMF solutions, BHMF is selectively produced at high HMF conversion and FE over Ag/Cu foams. The large surface area of 3D Ag/Cu foams, compared to their 2D counterparts, does not affect selectivity, but increases the rate of conversion and in turn the productivity. However, it would appear that the increase in the surface area is not enough to increase the efficiency in the conversion of more concentrated HMF electrolytes (0.05-0.50 M). The productivity of Ag/Cu is modified with electrocatalytic cycles.

1. Introduction

The electrochemical reduction or electrochemical hydrogenation (ECH) of 5-hydroxymethylfurfural (HMF) constitutes a fully sustainable route to produce fuels and chemicals.[1] The electrochemical route provides a path for the storage of renewable electric energy, avoids the use of H_2 at high pressure and can be operated at room temperature. The selectivity of the process depends on the reaction conditions and type of electrocatalyst.[1,2] For instance, the reductive ring opening producing 2,5-hexanedione occurs over Zn.[3] Acidic conditions lower the activation energy for HMF hydrogenation and hydrogenates the furan ring to tetrahydrofuran,[4] over CuNi electrodes dimethylfuran (DMF) is obtained by hydrogenolysis.[5] Operating in a neutral media, Na_2SO_4 and 0.05 M HMF, Ag shows the highest activity in 2,5-bis(hydroxymethyl)furan (BHMF) formation, by reduction of the aldehyde to the alcohol, with a selectivity > 85 %.[6] In basic medium (borate buffer pH = 9.2) with Ag modified Cu electrodes,[7] the process is more selective towards the production of BHMF, a precursor of polymers.[8] The morphology of the catalyst also plays a significant role. In the conversion of 0.02 M HMF over Ag/Cu in basic media solutions a 99% selectivity and faradaic efficiency (FE) are achieved with electrocatalysts prepared by galvanic displacement of Cu by Ag. The performance is explained considering the formation of dendrites that provided more effective binding sites for HMF and facilitated interfacial charge transfer. However, dealing with more concentrated HMF solutions resulted in low FE and yield mainly owing to a higher probability to form undesired products via dimerization or polymerization. For real deployment of the HMF electroreduction to BHMF in an industrial application, besides selectivity and faradaic efficiency, the process productivity should be largely increased. The largest productivities reported in the literature are still low for a practical application of the method.[7,9]

Nano-and macro-structuring largely increases the available surface area and therefore the productivity. Electrodes with nanoporous metal structures such as Ag displaced nanotextured Cu electrodes,[9] and Pd/VN hollow nanospheres sprayed into a bipolar membrane are successfully applied in the electrocatalytic hydrogenation of HMF into 2,5-bis(hydroxymethyl)-tetrahydrofuran (DHMTHF).[10] The unique morphology of the 3D hollow nanospheres provides materials with low resistance diffusion channels, facilitating diffusion and ion transport of the electrolyte.

Metallic open-cell foams increase the surface area per unit of volume, enhance mass and electron transfer and mechanical strength.[11] These materials are applied in water electrolysis[11,12] and CO_2 reduction,[13,14] besides they are gaining increasing interest in the electrochemical conversion of biomass derived compounds. Commercial Ni foams are supports of Ni-Boride,[15] Ni_2P nanoparticle arrays,[16] and Ni_3S_2 that are active in the electrocatalytic oxidation of HMF.[17] In the same process, home-made Cu foams are also applied.[18] These foams are generated by electrodeposition of Cu at high current densities,[19] H_2 bubbles develop and act as a geometric template for the metal plating (besides Cu also Ag foams can be prepared).[20] This method provides foams with a high roughness and surface area but with a gradient of pore sizes. On the other hand, commercial foams show a more regular structure, since they are produced starting from a polymeric template. When using foams as a support of the electrocatalytic phase, such as metallic nanoparticles required for the electroreduction of HMF, the coating procedure is of paramount importance to control the size, shape and distribution of the metallic particles. Electrodeposition is a single-step method largely used to produce additive-free nanoparticles where nanoparticles formation and deposition takes place simultaneously.[21] The properties of the nanoparticles can be tuned by electrochemical parameters such as deposition mode (pulsed or continued mode) and properties

of the electrolyte (concentration and type of precursors). Ag has been electrodeposited on Cu foams adjusting the cathodic potential applied and the deposition time to growth dendrites on the foam surface.[22]

The aim of this work is to increase the productivity in the electrocatalytic reduction of 5-hydroxymethylfurfrural to 2,5-bis(hydroxymethyl)furan in basic media (Scheme 1), using 3D electrocatalysts based on Cu open-cell foams coated by a layer of Ag particles through electrodeposition. For comparison purposes, bulk Ag and Cu foam electrodes (bare foams), as well as the foil Ag, Cu and Ag/Cu counterparts are studied. The stability of the electrocatalysts, hardly reported in the literature, is also investigated.

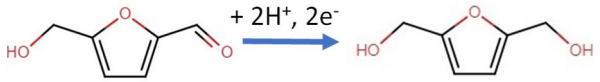

Scheme 1. Electrochemical hydrogenation of HMF to BHMF using H_2O as Hydrogen source.

2. Results and Discussion

2.1. Characterization of electrocatalysts

Ag and Cu bare foams are made by interconnected struts of about 50 µm diameter, forming 450 µm open-cells (Figure 1a, 1e). The surface of Cu foams is smooth, but cubic particles are observed in some regions (Figure 1b). XRD (Figure 1g) and Micro-Raman (Figure 1h) analyses suggest that these cubic particles are Cu_2O, which could be formed because of exposure to air of the material.[14] The surface of Ag foam resembles packed polyhedra that provide a high roughness (Figure 1f). Cubic Ag^0 is the only phase identified by XRD (Figure 1g). Ag and Cu foils have a striped surface (Figure S1), similar to that previously reported for Cu foils,[5] probably due to their manufacturing by rolling.

A template-free Ag^0 electrodeposition on Cu foams was performed by applying a -0.9 V vs SCE cathodic pulse for 25 s using an $AgNO_3$ solution under stirring to minimize convection and foster the replenishment of Ag^+ at the electrode-electrolyte interface. A homogeneous Ag film, made of aggregates (ca. 100 nm) of spherical Ag nanoparticles (ca. 10-20 nm), homogeneously cover the Cu foam surface (Figure 1c, c1, c2). The morphology of deposited Ag particles is different than in the work by Roylance et al.[7] where Ag dendrites are obtained. Herein, some Ag dendrites are only detected in the edges of some struts (more exposed sites of the foam) (Figure 1d), where the electrodeposition may be faster and limited by diffusion, conditions prone to dendritic particle growth. The length of the dendrites and size of the branches are in the 2 to 7 µm and 500 to 1000 nm range, respectively. Ag nanoparticles are highly interacting with the Cu foam, thus, besides an increase of the surface area of the active phase, a high electrical conductivity of the electrocatalyst is expected.

For comparison purposes, Cu foils are also coated by Ag keeping constant electrodeposition parameters; however, it should be considered that the shape of the support may modify the properties of the coating. Indeed, aggregates of spherical, needle-like and dendrite Ag particles deposit, forming a film thicker and less homogenous than in foams (Figure 2).

XRD patterns of Ag/Cu samples (foils and foams) show low intense cubic Ag^0 reflections, together with Cu^0 and Cu_2O reflections from the support (Figure 1g, S2a, S2b). The Raman bands of Cu_2O at 145, 215, 421, 528 and 619 cm^{-1} are identified in the spectra of both foils and foams (Figure 1h only shows the data for foam); moreover, a defective Cu_2O phase is suggested by the band at around 118 cm^{-1}, related to the Γ_{12}^- forbidden mode that is only active in presence of defects in Cu_2O.[23,24] It should be remarked that the oxidation of Cu support could take place during electrodeposition, due to the formation of a basic media by reduction of nitrates, which may explain the more intense Cu_2O bands in Ag/Cu than in Cu foam.

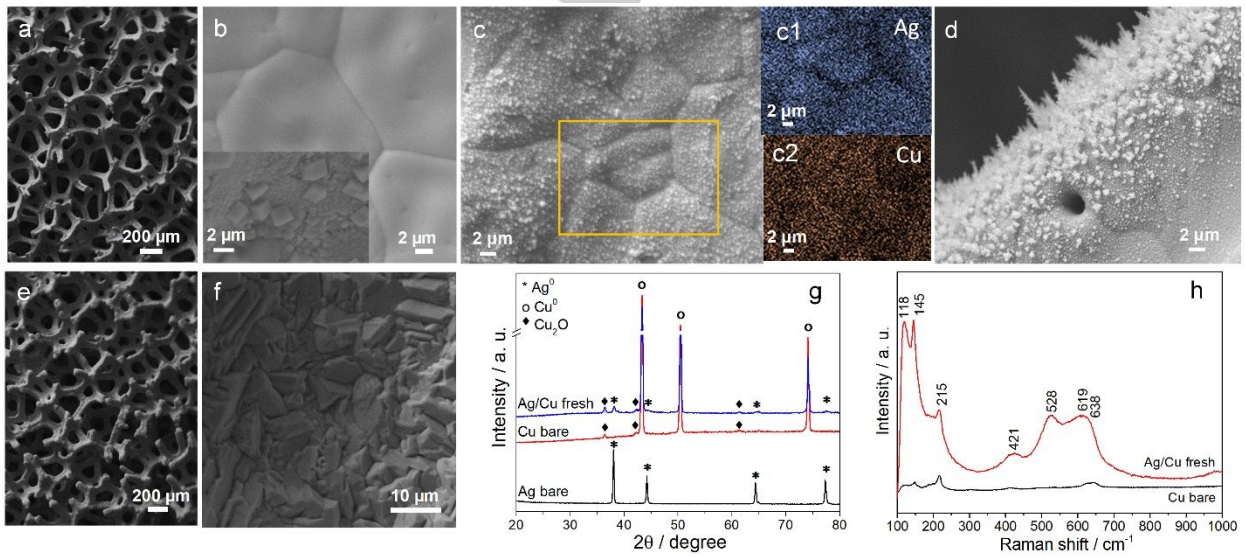

Figure 1. Characterization of foam electrodes. SEM images of Cu (a, b), Ag (e, f), and Ag/Cu (c, d). EDS Elemental maps of Ag/Cu foam measured in the highlighted zone in figure c (Ag - c1 and Cu – c2). XRD of Ag, Cu and Ag/Cu electrocatalysts (g). Micro-Raman spectra of Cu and Ag/Cu electrocatalysts (h).

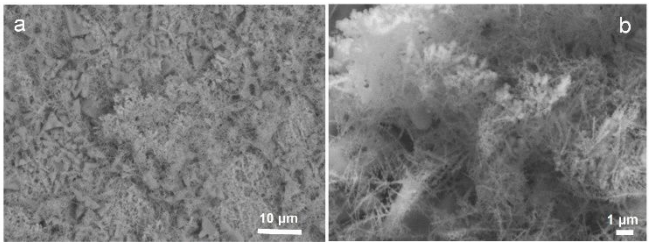

Figure 2. SEM images of an Ag/Cu foil electrocatalyst.

The electroactive surface area (EASA) of Ag/Cu and Ag foam and foil electrocatalysts is estimated by Pb underpotential deposition (Pb_{upd}) and subsequent stripping (Figure S3).[25] The charge corresponding to Pb stripping is used to calculate EASA values summarized in Table 1. The number of electroactive surface atoms exposed to the electrolyte is larger in Ag/Cu samples in comparison to Ag electrodes. EASA is three-fold larger for Ag/Cu than Ag regardless of the shape of the electrode, foam or foil. While a 3D support for Ag deposition also provides a three-fold EASA increase in comparison to the foil counterpart, i.e. 79 vs 23 cm^2 for the Ag/Cu foam and foil, respectively. It should be noted, however, that these measurements are challenging, UPD on Ag may have some limits to give absolute surface area values.[26] For instance, it has been reported that different catalysts may behave somewhat differently during Pb_{upd} and thus the appropriate potential range should be selected; moreover, it has been claimed that the underpotential deposition of Pb does not take place on Ag nanoparticles smaller than ca. 50 nm.[27,28] Last but not least, Cu is exposed on the surface of electrocatalysts and Pb_{upd} can occur on Cu,[26,29] indeed a surface area of 15 cm^2 was obtained for the Cu foam and 8 cm^2 for Cu foil (a value similar than for Ag foil).

Table 1. Electroactive surface areas (EASA) in cm^2 of foil and foam electrocatalysts.

EASA / cm^2	Cu	Ag	Ag/Cu
Foam	15	23	79
Foil	8	7	23

2.2. Electrochemical reduction of diluted HMF solutions

To investigate the role of the 3D support on the electrocatalytic reduction of HMF to BHMF, the research firstly focused on the conversion of diluted HMF solutions (0.02 M), making a comparison between foam- and foil-based electrocatalysts.

LSV experiments are performed in both borate buffer and borate buffer plus HMF electrolytes to analyze the activity of the electrocatalysts in the Hydrogen Evolution Reaction (HER) and HMF reduction, respectively (Figure 3). In the HER, Cu is more active than Ag foam in agreement with previous results,[7] water reduction starts at ca. 100 mV lower overpotential and the current density increases faster at more cathodic potentials (Figure 3a). The Ag/Cu catalyst behaves in between Ag and Cu electrodes. The LSV curve only shifts by around 30 mV towards more negative potentials in comparison to Cu (Figure 3a), and a lower current density is recorded afterwards, due to the poor activity of Ag in HER. It should be remarked that at potentials more anodic than -0.9 V vs SCE (-0.11 vs RHE) some peaks are recorded, which are related to the reduction of copper oxides. In particular a high intensity peak occurs at around -0.8 V vs SCE (-0.01 V vs RHE) in the first LSV in borate over Ag/Cu foam probably related to copper oxides developed during the preparation of the electrode, since it is absent in Cu foams. This peak is not observed in the following LSVs recorded at the same foam.

LSVs in electrolytes containing HMF are performed after LSVs in borate and rinsing the electrode with distilled water (see schema in Figure S4). The characteristic peak of HMF reduction is recorded at less cathodic potentials than HER for all the electrodes (Figure 3b).[7] The onset and minimum of the peak are quite similar for Ag and Cu foams; the difference in the shape of the peaks at more cathodic potentials than -1.2 V vs SCE (-0.41 V vs RHE) can be explained considering the higher activity of Cu in the HER. In that potential region both HER and HMF reduction contribute to the shape of peak but HER becomes dominant by moving to more negative potentials, therefore the current depends on the electroactivity of Ag and Cu foams for this reaction. Remarkably, the presence of Ag NPs on the surface of the Cu foam reduces the HMF reduction overpotential of about 60 mV, and a greater current density is measured.

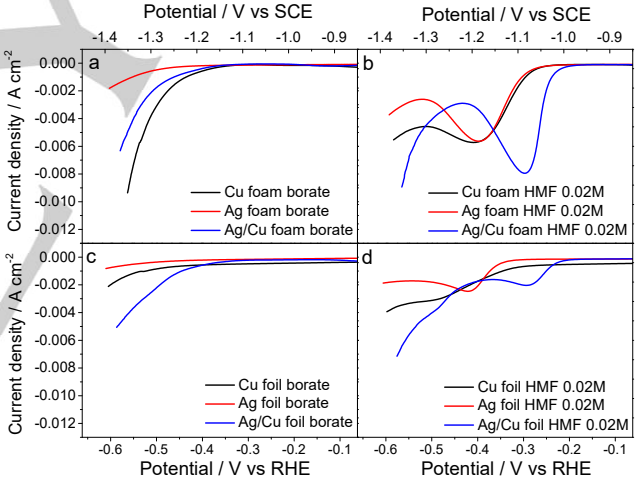

Figure 3. LSVs over Ag, Cu, and Ag/Cu foam and foil electrocatalysts in borate buffer (pH = 9.2) and 0.02 M HMF + borate buffer. (a, b) LSVs recorded at foams; (c, d) LSVs recorded at foils. Range: 0 - -1.4 V vs SCE. Scan rate: 1 mV/s for borate solutions and 5 mV/s for HMF containing solutions.

Unlike foams, the onset for the HER is quite similar for Ag and Cu foils (Figure 3c), though for the latter a higher current density is recorded. In Ag/Cu foil the current greatly increases in comparison to Ag and Cu foils. The HMF reduction onset is around 30 mV forward for foils than foams and the current densities exchanged decrease (Figure 3d). A low intensity peak is observed for Ag and Ag/Cu samples, while a shoulder is only recorded for Cu. The feature at around -1.27 V vs SCE (-0.48 V vs RHE) for the Ag/Cu sample has not been clearly identified yet, but may be related to the further reduction of species adsorbed on surface. When comparing foil- and foam-based

electrocatalysts not only differences in electroactive surface areas but also in mass transport phenomena could occur.

The onset of the reduction of HMF for Ag/Cu foams is in agreement with that reported by Roylance et al.[7] for Ag displaced on Cu foil. However, in the present work the minimum of the reduction peak is reached at more positive potentials and the current density is higher. It should be noted that we used the same electrolyte and scan rate as Roylance et al., but a smaller electrocatalyst geometric surface area and a larger electrolyte volume.[7] Hence, it would appear that the large surface area of the foams may improve the electroreduction of HMF.

The current-time transients obtained during electrolysis of 0.02 M HMF solutions at -1.3 V vs SCE (-0.51 vs RHE) over foam and foil electrocatalysts are shown in Figure 4a and 4b respectively. It should be noted that electrolysis are performed after LSVs in borate, and borate with HMF (Figure S4). The charge accumulated is 96.5 C (otherwise it is stated), corresponding to the charge to theoretically reduce all the 0.02 M HMF to BHMF considering a $2e^-$ process and 100% FE. The current density decreases during the first ca. 1800 and 300 s for Ag and Cu foams, respectively (Figure 4a). The limiting current density is greater for Cu; this behavior could be related to a higher HMF concentration in the plateau, because of a lower conversion in the first part of the curve or a higher contribution of the HER (vide infra). On the other hand, when Ag is deposited on the Cu foam the decrease in current density with time is slower and the limiting current density is not reached (Figure 4a). The largest surface area in Ag/Cu may provide an increase in the current and mass transfer, and therefore in the reaction rate at similar potentials.

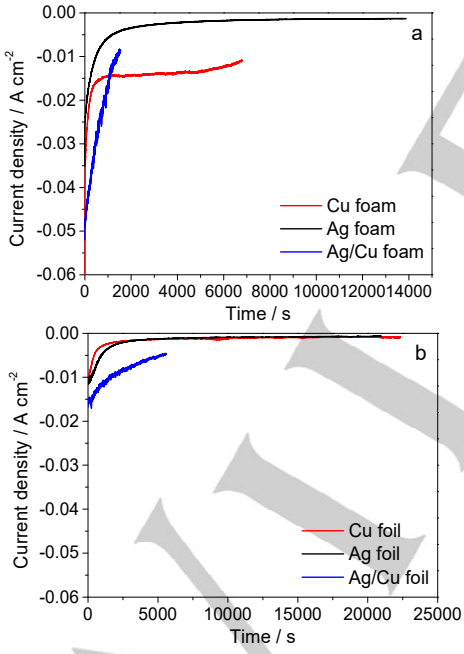

Figure 4. Current transients recorded during electrolysis experiments of 0.02 M HMF solutions in borate buffer (pH = 9.2) at -1.3 V vs SCE (-0.51 V vs RHE) over foam (a) and foil (b) electrocatalysts. The charge accumulated was 96.5 C with the exception of Ag and Cu foils that accumulated 60 C.

HMF conversion, selectivity in BHMF, FE and BHMF productivity for foam-based electrocatalysts are summarized in Figure 5. Ag outperforms Cu electrocatalyst in both HMF conversion and BHMF selectivity. For Ag, 93 % conversion and 75 % selectivity values are achieved. The low FE, ca. 69 %, is related to the formation of other HMF-derived byproducts, with a minor contribution of the HER, in agreement with the poor activity of Ag in the HER observed in the LSV. The Cu bare foam is less active and selective in the conversion of HMF to BHMF, and in turn FE is only 47 %. Conversely, BHMF productivity, referred as mmol h^{-1} cm^{-2}, is higher for Cu, despite conversion and selectivity are lower, due to the shorter time to accumulate the full charge, i.e. 13875 s vs 6890 s for the Ag electrode, related to the contribution of the HER. From these results it could be suggested that the rate of water reduction is faster over Cu than Ag, but also that HMF evolves to other by-products in a greater extent over Cu than Ag. Ag deposited on Cu foam (Ag/Cu) almost selectively converts HMF to BHMF (Sel. BHMF > 99%), while the conversion is below 100% (ca. 90%), which may be related to batch cell tests and the contribution of HER, i.e. once HMF is consumed HER becomes favored. It should be noted that in the Ag/Cu electrocatalyst, Ag homogeneously cover the foam surface but also Cu is exposed to the electrolyte. Hence, it could not be discarded that the electroactivity is related both to a higher electroactive surface area of Ag in Ag/Cu than in Ag electrocatalyst and to exposed Cu. However, unlike for Cu foam, BHMF selectivity is very high.

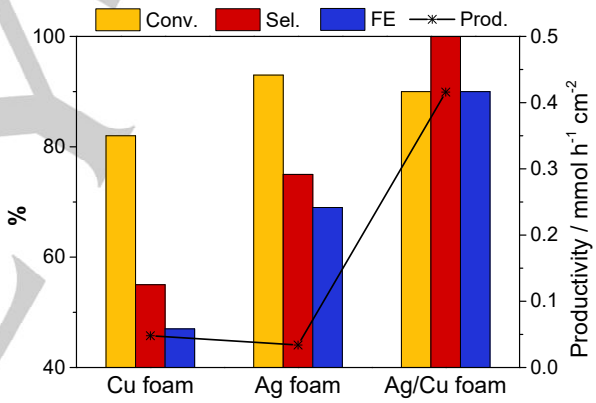

Figure 5. Results from electrolysis of a 0.02 M HMF solution in borate buffer (pH = 9.2) at -1.3 V vs SCE (-0.51 V vs RHE) over Ag, Cu, and Ag/Cu foam electrocatalysts. Charge accumulated 96.5 C.

After electrolysis, the electrochemical behavior of foams, rinsed with water and acetonitrile, in the HER and HMF reduction is evaluated again through LSV in both borate and borate plus HMF (Figure S5a). The curves before and after electrolysis are slightly modified in terms of onset and current density recorded, it could be related to the position of the electrodes but also to modifications in the surface of the electrocatalyst.

For comparison purposes the results obtained during electrolysis over foil counterparts are displayed in Figure 4b and Table 2. The main effect of using a foil-based electrode is a decrease in the current recorded and therefore in the duration of the experiments (Figure 4b). Both Ag and Cu electrocatalysts reach a limiting current density of 0.001 A cm^{-2} in the first part of the experiments (ca. 2500 s); since the process was slow it was not possible to accumulate 96.5 C and the reaction was stopped at 60 C. Hence, an accurate comparison between Ag and Cu foil and foam electrocatalysts performance cannot be made;

however, it should be noted that selectivities are similar to those obtained over foam electrocatalysts (Table 2). On the other hand, for Ag/Cu foil, like for the foam counterpart, the current density exponentially decreases with the time and it does not reach the limiting current. Ag nanoparticles on the Cu foil support allows to selectively convert HMF into BHMF (Sel. BHMF = 98%). Conversely, conversion and FE are low, probably due to the contribution of the HER. Consequently, productivity also largely decreases in comparison to foams, e.g. 0.108 vs 0.416 mmol h^{-1} cm^{-2} for foil and foam, respectively. These results highlight the advantages of using electrodes based on open-cell foams with a high surface area electrode to increase the efficiency.

Table 2. Results from electrolysis of a 0.02 M HMF solution in borate buffer (pH = 9.2) at -1.3 V vs SCE (-0.51 V vs RHE) over Ag, Cu, and Ag/Cu foil electrocatalysts.

Sample	Conv. HMF / %	Sel. BHMF / %	FE / %	BHMF Productivity / mmol h^{-1} cm^{-2}
Cu foil[a]	51	55	45	0.012
Ag foil[a]	57	74	68	0.019
Ag/Cu foil[b]	69	98	67	0.108

[a] Charge accumulated 60 C [b] Charge accumulated 96.5 C

To check the stability of Ag/Cu foam catalyst two more electrocatalytic cycles were performed over the same sample; every cycle includes (Figure S4): i) LSV in borate; ii) LSV in borate plus HMF; iii) electrolysis at constant potential; iv) LSV in borate; v) LSV in borate and HMF. In between experiments electrodes were rinsed with water and acetonitrile. Two different samples were investigated obtaining similar results. LSVs are slightly modified before and after electrolysis (Figure S5a), and the profile of current transients also changes (Figure S5b). The time required to collect the charge to selectively convert all the HMF to BHMF increases from the first to the third cycle, but the electrocatalytic performance in terms of conversion and selectivity and in turn FE are kept constant (Table 3). It would appear that the kinetics of HMF reduction are modified along the cycles, consequently influencing on the BHMF productivity. The changes in the shape of the current density transients can be related to mass transfer and activity of the catalyst. This behavior is under investigation.

Table 3. Results from electrolysis of a 0.02 M HMF solution in borate buffer (pH = 9.2) at -1.3 V vs SCE (-0.51 V vs RHE) over an Ag/Cu foam electrocatalyst. The numbers indicate the repetition of the test during the catalytic cycle, test "R" is the test performed after HMF 0.50 M. Charge: 96.5 C

Test	Conv. HMF / %	Sel. BHMF / %	FE. / %	BHMF Productivity / mmol h^{-1} cm^{-2}
1	90	100	94	0.416
2	92	99	93	0.357
3	93	100	99	0.291
R	90	96	91	0.263

The evolution of the electrochemical process with time is also investigated by analyzing aliquots of the electrolytic solution at 20, 40, 60, 80 and 96.5 C. A small volume (ca. 0.7 mL) is withdrawn with a pipette from the electrolyte assuming that the composition of the solution is homogeneous because of effective stirring; the current transient curve is not modified during the electrolyte withdrawn. HMF conversion steadily increases with the charge accumulated, while changes in selectivity are less remarkable (Table 4). For instance, after 20 C collected, conversion is 27 % and BHMF selectivity is already 89 %, by further accumulating 40 C conversion doubles and selectivity reaches a 94 %. Productivity decreases with the accumulated charge, starting from 0.708 mmol h^{-1} cm^{-2} after 20 C to 0.289 mmol h^{-1} cm^{-2} at the end of test, due to the decrease of HMF concentration with the reaction time in the batch cell. The same trend is reported in the literature for Ag/Cu flat electrodes in the reduction of HMF 0.02 M at a similar potential,[7,9] but foam electrocatalysts in this work show a higher productivity for all the accumulated charges. For instance, Roylance et al. reported a 0.127 mmol h^{-1} cm^{-2} productivity at 20 C (37 % BHMF conversion and 99% FE),[7] while the value obtained by Zhang et al. is 0.052 mmol h^{-1} cm^{-2} (28 % BHMF conversion and 100 % FE).[9]

Table 4. Results from electrolysis of a 0.02 M HMF solution in borate buffer (pH = 9.2) at -1.3 V vs SCE (-0.51 V vs RHE) over Ag/Cu foam electrocatalyst accumulating different charge.

Charge / C	20	40	60	80	96
Conv. HMF/ %	27	46	65	83	93
Sel. BHMF / %	89	94	95	95	99
BHMF Productivity / mmol h^{-1} cm^{-2}	0.708	0.583	0.484	0.376	0.291

2.3. Electrochemical reduction of concentrated HMF solutions

The effect of the HMF concentration on the electroactivity of Ag/Cu foam is investigated. LSVs and electrolysis are performed in 0.05, 0.10 and 0.50 M HMF solutions under similar conditions and using both freshly prepared electrocatalysts and the same Ag/Cu catalyst tested above to investigate the stability of the electrocatalyst. The sequence of analyses performed with the Ag/Cu catalyst is summarized in Figure S4.

More concentrated HMF electrolytes do not significantly shift the onset in the LSV (except for 0.50 M that occurs at around 50 mV lower overpotential), while increase the faradaic current recorded (Figure 6a), but not proportionally to the HMF concentration. This behavior could be related to the adsorption of organic compounds on the surface of the electrode, likewise for furfural on Cu electrodes,[30] or due to the competition between HER and HMF reduction.[6] At high overpotentials the kinetics of HER increases faster than the kinetics of aldehyde group reduction.[31] Moreover, for the 0.50 M sample a mass transfer limited plateau is observed.

Electrolysis were performed after LSV in borate and borate plus HMF accumulating the charge required to convert all the HMF to BHMF with the exception of the 0.50 M solution, where only the charge to convert 52 % HMF to BHMF (1152 C) was accumulated because of time issues. The increase in the concentration from 0.02 to 0.10 M reduces the current density exchanged in the first part of electrolysis experiments and enlarges the tests, suggesting a deactivation of the electrocatalyst (Figure 6b). It should be remarked that current transients are slightly affected by the "history" of the electrocatalyst (Figure S6). Namely, for Ag/Cu foam fresh samples the current starts between 45 and 55 mA cm^{-2}, and decreases almost linearly until the end of the test, while for the Ag/Cu sample already tested, the current density at the beginning is lower (around 40 mA/cm^{-2}) and reaches the limiting current density of about 2.5 mA cm^{-2}.

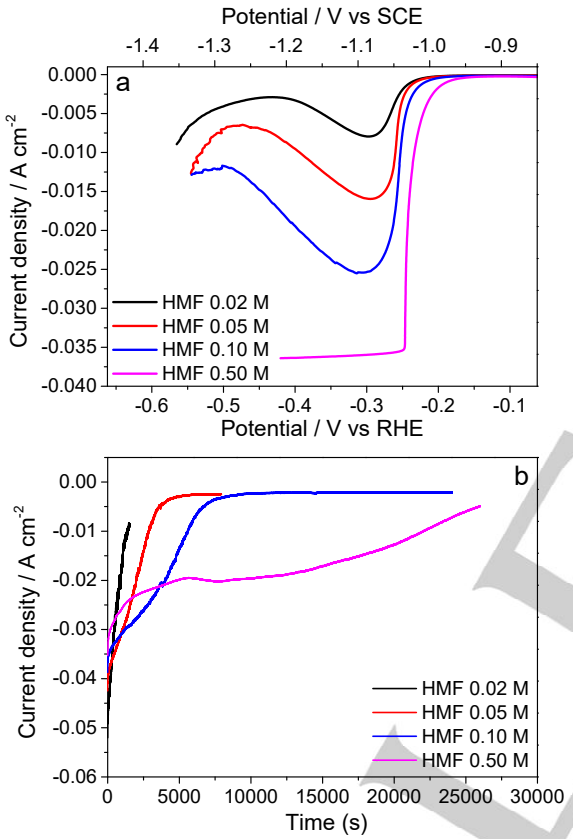

Figure 6. LSVs (a) and current transients during electrolysis (b) over Ag/Cu foam used electrocatalyst immersed in electrolytes with different HMF concentration. (a) Range: 0 - -1.4 V vs SCE; scan rate: 5 mV s^{-1}. (b) -1.3 V vs SCE (-0.51 V vs RHE); charge accumulated: 96.5 C (0.02 M); 241.2 C (0.05 M); 482.4 C (0.10 M); 1152 C (0.50 M).

HMF conversion increases in more concentrated electrolytes (Figure 7), reaching almost 100 % values, even in the 0.50 M electrolyte where the charge accumulated was only the half one to convert HMF to BHMF (1152 C instead of 2412 C). BHMF selectivity achieves an acceptable 83 % with the 0.05 M solution, but it drops to only 13 % in a 10-fold more concentrated electrolyte. The lower FE values seem to be mainly related to the formation of byproducts rather than to the contribution of the HER. The poor selectivity in the conversion of HMF into BHMF and the long times required to accumulate the charge during the electrolysis of concentrated solutions provoke a large decrease in productivities, unlike for the electrocatalytic hydrogenation of benzaldehyde, where the increase in the concentration enhances productivity.[32] Moreover, the different times to accumulate the charge for Ag/Cu fresh and Ag/Cu tested above explained, explain that the productivities are greater for the former, regardless of the HMF concentration (in Table S1 a comparison with the 0.05 M electrolyte is shown).

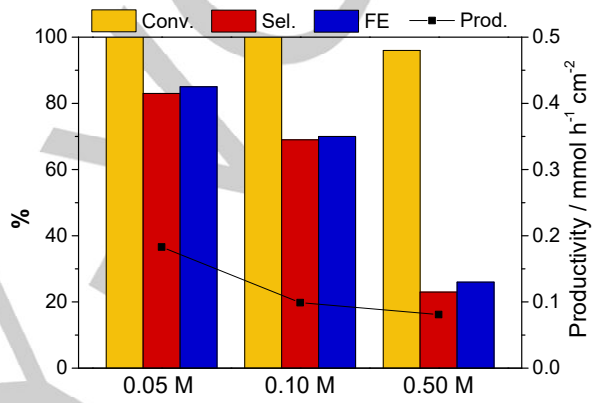

Figure 7. Results from electrolysis at constant potential over the same Ag/Cu foam used electrocatalyst of electrolytes with different HMF concentrations. Potential: at -1.3 V vs SCE (-0.51 V vs RHE). Charge accumulated: 96.5 C (0.02 M); 241.2 C (0.05 M); 482.4 C (0.10 M); 1152 C (0.50 M).

To further evaluate the stability of the Ag/Cu used catalyst after the electrocatalytic test with HMF 0.50 M electrolyte, the first test with HMF 0.02 M was replicated, named "R test" in Table 3. Results are rather similar in comparison with the previous test at 0.02 M (entry test 3), with a slight decrease in the selectivity and in turn in FE; though productivities are in line, indeed, current transients of both tests superimposed (Figure S7c). Taking also into account, the changes in the LSVs in borate and borate plus HMF (Figure S7a, b) along the tests, it would appear that some modifications, conditioning, on the surface of the electrocatalyst occur in the first part of the experiments with 0.02 M solutions. SEM images and Ag and Cu element maps from EDS of this sample after 35 h tests does not show any significant change either on the morphology of the coating or Ag distribution (Figure 8). The XRD pattern confirms the reduction of the catalyst during tests, the Cu_2O reflections are not observed (Figure S8). The analysis of the solution by ICP indicates that Ag does not leach, or if something is leached its amount is below the detection limit of the instrument.

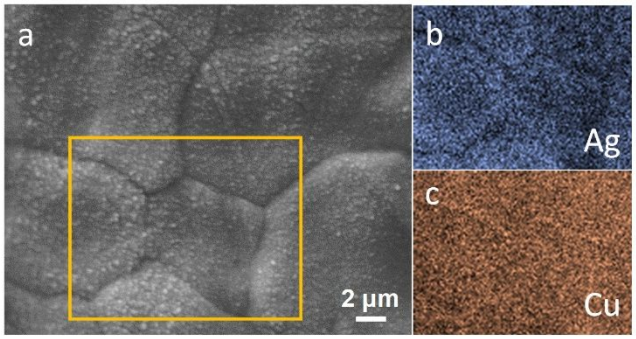

Figure 8. SEM image of an Ag/Cu foam after catalityc tests (a) and EDS elemental maps: Ag (b) and Cu (c).

2.4. Identification of byproducts

In HPLC chromatograms some unknown peaks are observed, the most intense one being close to the BHMF peak (Figure S9). To go insight into the formation of byproducts GC-MS and ESI-MS analyses of the solutions after electrolysis were performed.

GC-MS analyses evidence the formation of 5-methylfurfuryl alcohol and 5-methyl furfural (Figure S10) and the presence of high molecular products. 5-methylfurfuryl alcohol has been previously related to the presence of Cu;[9] however, making a comparison between our work and the previous one is not straightforward because herein a larger volume of electrolytic solution is used and the size of the catalyst is different. The formation of dimers and oligomers as by-products is reported by Roylance et al. however the compounds are not identified.[7], while very recently Chadderdon et al reported the formation of 5,5′-Bis(hydroxymethyl) hydrofuroin.[33]

To further investigate the formation of higher molecular compounds, ESI-MS analysis of the most concentrated 0.50 M solution (achieving the lowest BHMF selectivity) after electrolysis and extraction with acetonitrile was carried out. The spectra in Figure S11 reveals the presence an intense peak corresponding to a 254 mass attributed to 5,5′-Bis(hydroxymethyl) hydrofuroin. Higher molecular weight compounds are also identified, related to the formation of oligomers and polymers. The extracted organic phase was also analyzed by HPLC; the chromatogram shows a peak at a retention time similar to the unknown peak previously described in the reaction mixture chromatogram (Figure S10). Hence, it could be concluded that this peak is related to the 5,5′- Bis (hydroxymethyl) hydrofuroin, and that is one of the most abundant byproducts. Currently we are not able to correlate the area of the peak with the concentration of the hydrofuroin. However, an estimation of the hydrofuroin formation is made by analyzing the area of the peak normalized to HMF conversion (Table 4). The hydrofuroin linearly correlates with the concentration of HMF in the electrolyte.

Table 4. Area of the peak of the 5,5′-Bis(hydroxymethyl) hydrofuroin divided by the conversion obtained in electrolysis of 0.02, 0.05, 0.10 and 0.50 M HMF in borate buffer (pH = 9.2) at -1.3 V vs SCE (-0.51 V vs RHE) over an Ag/Cu foam electrocatalyst.

HMF conc.	0.02 M[a]	0.05 M[b]	0.10 M[c]	0.50 M[d]
$\frac{\text{Area hydrofuroin}}{\text{Conv. HMF}}$	74	602	1019	1773

[a] 96.5 C; [b] 241.2 C; [c] 482.4 C; [d] 1152 C

A change in HMF surface coverage and HER contribution occurs with the increase in HMF conversion, therefore the aldehyde reduction proceeds through a one-electron process producing a radical that dimerizes to the hydrofuroin (Scheme 2) or that further polymerizes as previously observed for furfural and benzaldehyde[30,34-36] and recently reported for HMF.[33] This mechanism explains the full HMF conversion despite the charge accumulated is only 1152 C, moreover the presence of oligomers or polymers supports the deactivation of the electrocatalyst surface.

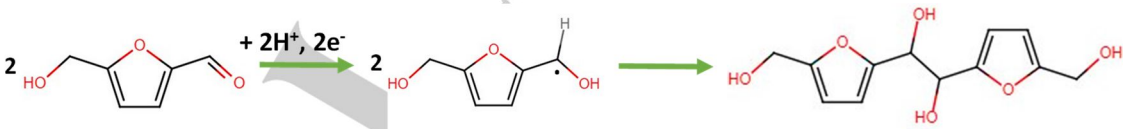

Scheme 2. Route for the formation of 5,5′-Bis(hydroxymethyl) hydrofuroin.

3. Conclusion

The combination of electrodeposited Ag nanoparticles and Cu open-cell foams provides optimum performances in the fully selective electrochemical conversion of very diluted HMF electrolytes to BHMF in basic media. Most importantly, productivity is largely increased in comparison to their 2D foil counterpart. In particular, the increase of the electroactive surface area in 3D foam-based electrodes does not have any effect on the selectivity of the process but on the rate of HMF conversion.

However, the increase in the surface area in 3D electrocatalysts is not enough to overcome the challenge of the electrocatalytic reduction of concentrated HMF electrolytes. Indeed, over Ag deposited on Cu foams, selectivity drops by increasing the HMF concentration (0.05-0.50 M), since a radical mechanism forming a hydrofuroin is prevalent.

Last but not least, the conditioning of the electrocatalyst seems to occur. The electrocatalytic activity, in terms of current density exchanged, is modified during the first set of tests. A longer time is necessary to accumulate the charge, but conversion and selectivities are unaltered, consequently productivity decreases.

However, after the conditioning the activity seems to be stable for around 35 h of electrocatalytic tests.

Experimental Section

Materials and chemicals

Ultrapure water (18 MΩ.cm) was used for the preparation of all aqueous solutions. Cu foil (0.25 mm thickness, 99.98%) and Ag foil (0.127 mm thickness, 99.99%) were purchased from Sigma-Aldrich and Alfa-Aesar, respectively. Cu and Ag foams were supplied by Alantum. Sodium hydroxide (≥98%) was purchased from Sigma-Aldrich. Boric acid (≥99.5%) and silver nitrate (99.9+%) were purchased from Alfa Aesar while 5-hydroxymethylfurfural (99%) was purchased from AVA Biochem.

For the determination of Electroactive Surface Area (EASA), Lead Nitrate (99.5%), Sodium Potassium Tartrate (99%) and Sulfuric acid (96%) were purchased from Sigma-Aldrich.

To assist in High Performance Liquid Chromatography (HPLC) method development, standard calibration, and product identification, 2,5-bis(hydroxymethyl)furan was purchased from Toronto Research Chemicals.

All chemicals were used without further purification.

Preparation of electrocatalysts

Foam electrodes were prepared by cutting Cu and Ag foam panels of 1.6 mm thickness and 450 µm cell size into 10 mm x 10 mm pieces (geometric surface area 2.64 cm^2). Cu and Ag foils were cut into 10 mm x 15 mm pieces, the actual exposed area is 10 mm x 10 mm (geometric surface area 2 cm^2). Cu or Pt wires were attached to the electrodes to enable connection to the potentiostat. Before the use, the electrodes were cleaned by washing with 2-propanol and water, followed by immersing in 1 M HCl for 5 min to remove surface oxides, and water to remove HCl.

Electrochemical measurements were controlled by a potentiostat/galvanostat Metrohm Autolab PGSTAT204, equipped with NOVA software.

The deposition of the Ag was performed by electrodeposition on Cu foams or foils in a single-compartment three-electrode cell. Foams or foils were the working electrodes (WE), while a saturated calomel electrode (SCE) and a Pt wire were the reference electrode (RE) and counter electrode (CE), respectively. The RE was placed close to surface of the WE and both of them were located in the center of the CE. The electrodeposition was performed by applying a 25 s pulse at -0.9 V vs SCE (-0.11 vs RHE), using 25 mL of 5.0 mM $AgNO_3$ aqueous solution electrolyte under magnetic stirring of 500 rpm. After electrodeposition, the catalysts were rinsed gently with ethanol and water.

Characterization techniques

The X-ray diffraction (XRD) analysis was carried out using a PANalytical X'Pert diffractometer equipped with a copper anode (λ_{mean} = 0.15418 nm) and a fast X'Celerator detector. Wide-angle diffractogram was collected over 2θ range from 3 to 80° with a step size of 0.067° and counting time per step 60.95 s.

The surface morphology of the electrodes was examined by Scanning electron microscopy/energy dispersive spectroscopy (SEM/EDS) using an EP EVO 50 Series Instrument (EVO ZEISS) equipped with an INCA X-act Penta FET® Precision EDS microanalysis and INCA Microanalysis Suite Software (Oxford Instruments Analytical). The accelerating voltage was 20 kV and the spectra were collected in duration 60 s.

Micro-Raman spectra were recorded with a Renishaw Raman Invia spectrometer configured with a Leica DMLM microscope using Ar^+ laser source (λ = 514.5 nm, P_{out} = 30 mW considering the decrease in power due to the plasma filter). In each measurement, the laser power was set by 10% of the source and the signal was accumulated by 4 individual spectra with an acquisition time of 10 s.

Electrochemical measurements

All electrochemical experiments were conducted in a three-electrode three-compartment cell separated by glass frits. Working electrodes were Ag and Cu foils and foams and Ag coated on Cu foams and foils placed in the central compartment. Counter electrodes were Pt wires placed in the side compartments. A saturated calomel electrode (SCE) was used as reference electrode. The reference electrode was in electrolytic contact with the main compartment via a Luggin capillary. All potentials were reported vs SCE and RHE (V vs RHE = V vs SCE + 0.244V + 0.0591pH). The cell was immersed in a thermostated water bath at 25°C. The current interrupt approach was used to determine the R_u, applying a potential pulse of 1 mV for 2 ms. The iR drop for all the LSVs were compensated after measurements, instead the constant-potential electrolysis were performed without compensation.

In the working electrode compartment, electrolytes were 25 mL of 0.5 M borate buffer aqueous solution (pH 9.2) with and without HMF. The 25 mL of electrolyte is required to ensure that the foam is completely wet and the solution well mixed HMF concentrations were 0.02, 0.05, 0.10 and 0.50 M. In the counter electrode compartments the anolyte was a 0.5 M borate buffer solution (pH 9.2) with 0.5 M sodium sulfite. [7]

The electrochemical characterization of the catalysts was performed by linear sweep voltammetry (LSV) recorded in a 0.5 M borate buffer solution (pH 9.2) with and without HMF. The solutions were purged with N_2 to remove dissolved oxygen before the measurements, keeping N_2 flow in the open-space during LSV. The potential was varied from 0 to −1.4 V vs SCE (from 0.79 to -0.61 vs RHE) at a scan rate of 1 mV s^{-1} without HMF and 5 mV s^{-1} with HMF. The slowest scan rate in the LSV without HMF was chosen to ensure the reduction of the electrocatalyst.

The estimation of the electroactive surface area of electrodes was carried out measuring the deposition/dissolution charge of lead underpotential deposition (UPD), comparing with the response of polished Ag foil. Ag foil with a dimension of 10 mm x 10 mm was abraded with emery paper of 300, 600, 800, 1200, 2500 grit and finally polished with 50 nm colloidal silica, then the material was rinsed with water and acetone. The measurements of EASA were performed recording a cyclic-voltammetry (CV) in

a single compartment three-electrode cell described in section 2.2. Cyclic voltammograms were recorded between 0 and -0.6 V vs SCE (from 0.79 to -0.19 vs RHE), with a scan rate of 50 mV s^{-1}. The electrolyte was an aqueous solution of 0.10 M sodium potassium tartrate containing 0.01 M H_2SO_4 and $3*10^{-4}$ M $Pb(NO_3)_2$.[26]

Electrocatalytic hydrogenations were performed potentiostatically at -1.3 V vs SCE (-0.51 vs RHE) using deaerated electrolytes with different HMF concentrations (0.02, 0.05, 0.10 and 0.50 M) and flushing N_2 in the overhead of the working electrode compartment. The experiments were performed under stirring of the solution with a magnetic bar at a rotating speed of 1000 rpm. The effect of the stirring rate was preliminary investigated; a test at 500 rpm showed lower conversion but quite similar selectivity and FE. Increasing the stirring the vortex can worsen the mass transfer, decreasing the catalytic performance.

The catalytic cycle is composed by a sequence of LAV in borate and borate plus HMF, electrolysis at constant potential and then the first two LSVs are repeated. LSV performed just before of HMF electroreduction to ensure reduction of any surface oxide species to minimize Faradaic loss during the process, instead after the catalytic test allows to check for any change in the electrocatalysts after reaction. Once the first cycle was completed a new electrolysis could be immediately performed, starting a new catalytic cycle (Figure S4). This sequence was replicated for all investigated HMF concentration.

The reactions were carried out under total HMF conversion conditions, which were obtained through the transfer of the charge necessary to convert all HMF in solution into BHMF (i.e. through a 2 e- process). At the end the solutions were collected and analyzed with HPLC. All the measurements were performed in three replicates. The geometric surface areas of the electrodes were considered for calculating current densities.

Product Analysis

Quantitative analysis of the product concentrations in the electrolytes was conducted by means of a HPLC Agilent 1260 Infinity Series provided with Cortecs T3 2.4 µm (4.6 x 100 mm) operating at 30 °C, equipped with an autosampler (injection volume 1 µL) and a Diode-Array Detector set at 284 nm for the identification of HMF and 223 nm for the identification of BHMF. The analyses were performed with gradient elution in three steps: isocratic conditions for 6 minutes, with eluent composed of CH_3CN/H_2O 10/90 v/v ratio; gradient elution for 5 minutes until a CH_3CN/H_2O 50/50 elution ratio was obtained; gradient elution for 4 minutes until a CH_3CN/H_2O 70/30 elution ratio was obtained. The flow rate was 0.7 mL min^{-1}.

Conversion, selectivity, faradaic efficiency (FE) and BHMF productivity were calculated with the following equations:

$$X_{HMF}(\%) = \frac{\text{mol}_{\text{HMF consumed}}}{\text{mol}_{\text{HMF initial}}} \text{x}100$$

$$S_{BHMF}(\%) = \frac{\text{mol}_{\text{BHMF formed}}}{\text{mol}_{\text{HMF consumed}}} \text{x}100$$

$$\text{FE}\ (\%) = \frac{\text{mol}_{\text{BHMF formed}}}{\text{total charge passed}/(\text{Fx}2)} \text{x}100$$

where F is the Faraday constant

$$\text{BHMF productivity} = \frac{\text{mmol BHMF formed}}{\text{reaction time (h)} * \text{area (cm}^2\text{)}}$$

The area corresponds to the geometric area of electrodes, 2.64 cm^2.

The identification of some by-products was performed by Gas Chromatography- mass spectrometry (GC-MS) and electrospray ionization mass spectrometry (ESI-MS). The GC-MS was an Agilent 6890N series instrument coupled with a mass spectrometer Agilent technologies 5973 Inert, with manual injection, and with a capillary column Agilent HP5, composed by (5%-Phenyl)-methylpolysiloxane. The identification of the products was made via MSD Chemstation software including the standard NIST database. The ESI-MS instrument was a Waters micromass ZQ 4000, with manual injection. For GC-MS and ESI-MS analyses an amount of the reaction solution was extracted for three times with acetonitrile. Then both the aqueous and organic phases were analyzed.

Acknowledgements

The financial support from AlmaIdea Project from the University of Bologna is acknowledged. The authors acknowledge Alantum for supplying the foams.

Keywords: 5-Hydroxymethylfurfural •2,5-Bis(hydroxy methyl)furan • Electrocatalyst • Ag/Cu • Foam

[1] Y. Kwon, K. J. P. Schouten, J. C. van der Waal, E. de Jong, M. T. M. Koper, *ACS Catal.* **2016**, *6*, 6704−6717.
[2] S. Chen, R. Wojcieszak, F. Dumeignil, E. Marceau, S. Royer, *Chem. Rev.* **2018**, *118*, 11023−11117.
[3] J. J. Roylance, K.-S. Choi, *Green Chem.* **2016**, *18*, 2956–2960.
[4] Y. Kwon, Y. Y. Birdja, S. Raoufmoghaddam, M. T. M. Koper, *ChemSusChem* **2015**, *8*, 1745–1751.
[5] Y.-R. Zhang, B.-X. Wang, L. Qin, Q. Li, Y.-M. Fan, *Green Chem.* **2019**, *21*, 1108–1113.
[6] Y. Kwon, E. De Jong, S. Raoufmoghaddam, M. T. M. Koper, *ChemSusChem* **2013**, *6*, 1659–1667.
[7] J. J. Roylance, T. W. Kim, K.-S. Choi, *ACS Catal.* **2016**, *6*, 1840−1847.
[8] L. Hu, J. Xu, S. Zhou, A. He, X. Tang, L. Lin, J. Xu, Y. Zhao, *ACS Catal.* **2018**, *8*, 2959−2980.
[9] L. Zhang, F. Zhang, F. C. Michel, A. C. Co, *ChemElectroChem* **2019**, *6*, 4739–4749.
[10] S. Li, X. Sun, Z. Yao, X. Zhong, Y. Cao, Y. Liang, Z. Wei, S. Deng, G. Zhuang, X. Li, J. Wang, *Adv. Funct. Mater.* **2019**, *29*, 1904780 DOI: 10.1002/adfm.201904780
[11] W. Zhu, R. Zhang, F. Qu, A. M. Asiri, X. Sun, *ChemCatChem* **2019**, *9*, 1721-1743.
[12] D. Wang, J. Li, H. Xu, Y. Zhao, *Electrochim. Acta* **2019**, *316*, 8-18.
[13] X. An, S. Li, A. Yoshida, T. Yu, Z. Wang, X. Hao, A. Abudula, G. Guan, *ACS Appl. Mater. Interf.* **2019**, *11*, 42114−42122.
[14] A. Dutta, M. Rahaman, N. C. Luedi, M. Mohos, P. Broekmann, *ACS Catal.* **2016**, *6*, 3804−3814.
[15] S. Barwe, J. Weidner, S. Cychy, D. M. Morales, S. Dieckhçfer, D. Hiltrop, J. Masa, M. Muhler, W. Schuhmann, *Angew. Chem. Int. Ed.* **2018**, *57*, 11460 –11464.
[16] B. You, N. Jiang, X. Liu, Y. Sun, *Angew. Chem. Int. Ed.* **2016**, *55*, 9913 –9917.
[17] B. You, X. Liu, N. Jiang, Y. Sun, *J. Am. Chem. Soc.* **2016**, *138*, 13639−13646.
[18] D.-H. Nam, B. J. Taitt, K.-S. Choi, *ACS Catal.* **2018**, *8*, 1197−1206.

[19] H. C. Shin, M. L. Liu, *Chem. Mater.* **2004**, *16*, 5460−5464.
[20] Q. H. Low, N. W. X. Loo, F. Calle-Vallejo, B. S.Yeo, *Angew. Chem. Int. Ed.* **2019**, *58*, 2256 –2260.
[21] S. E. F. Kleijn, S. C. S. Lai, M. T. M. Koper, P. R. Unwin, *Angew. Chem. Int. Ed.* **2014**, *53*, 3558 – 3586.
[22] F. Urbain, P. Tang, N. M. Carretero, T. Andreu, J. Arbiol, J. R. Morante, *ACS Appl. Mater. Interf.* **2018**, *10*, 43650−43660.
[23] Y. Deng, A. D. Handoko, Y. Du, S. Xi, B. S. Yeo, *ACS Catal.* **2016**, *6*, 2473−2481.
[24] M. Ivanda, D. Waasmaier, A. Endriss, J. Ihringer, A. Kirfel, W. Kiefer, *J. Raman Spectrosc*. **1997**, *28*, 487-493.
[25] G. K. H. Wiberg, K.J.J. Mayrhofer, M. Arenz, *Fuel Cells* 10, **2010**, No. 4, 575–581.
[26] L. Mattarozzi, S. Cattarin, N. Comisso, P. Guerriero, M. Musiani, E. Verlato, *Electrochim. Acta* **2016**, *198*, 296–303.
[27] F.W. Campbell, R.G. Compton, *Int. J. Electrochem. Sci.* **2010**, *5*, 407–413.
[28] O.A. Oviedo, L. Reinaudi, E.P.M. Leiva, *Electrochem. Commun.* **2012**, *21*, 14-17.
[29] G. Y. Wu, S.-E. Bae, A. A. Gewirth, J. Gray, X. D. Zhu, T. P. Moffat, W. Schwarzacher, *Surf. Sci.* **2007**, *601*, 1886–1891.
[30] P. Nilges, U. Schröder, *Energy Environ. Sci.* **2013**, *6*, 2925–2931.
[31] C. J. Bondue, Marc T. M. Koper, *J. Am. Chem. Soc.* **2019**, *141*, 12071−12078.
[32] J. A. Lopez-Ruiz, U. Sanyal, J. Egbert, O. Y. Gutiérrez, J. Holladay, *ACS Sustainable Chem. Eng.* **2018**, *6*, 16073−16085.
[33] X. H. Chadderdon, D. J. Chadderdon, T. Pfennig, B. H. Shanks W. Li, *Green Chem.* **2019**, *21*, 6210-6219.
[34] X. H. Chadderdon, D. J. Chadderdon, J. E. Matthiesen, Y. Qiu, J. M. Carraher, J.-P. Tessonnier, W. Li, *J. Am. Chem. Soc.* **2017**, *139*, 14120−14128.
[35] S. Jung, E. J. Biddinger, *Energy Technol.* **2018**, *6*, 1370 – 1379.
[36] P. Parpot, A.P. Bettencourt, G. Chamoulaud, K.B. Kokoh, E.M. Belgsir, *Electrochim. Acta* **2004**, *49*, 397–403.

Entry for the Table of Contents

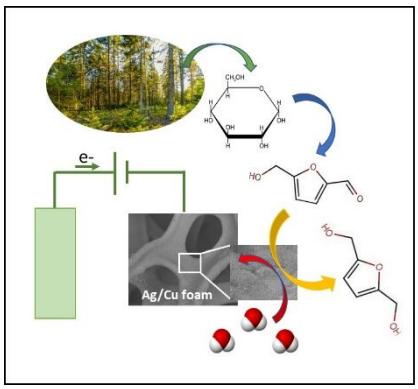

Not only the electroactive surface matters. 3D electrocatalysts made by Ag nanoparticles electrodeposited on Cu open-cell foams largely increases the productivity in the selective conversion of diluted 5-hydroxymethylfurfural to 2,5-bis(hydroxymethyl)furan. While the large electroactive surface area is not enough to avoid the hydrofuroin byproduct formation.

Supplementary Information

Ag electrodeposited on Cu open-cell foams for the selective electroreduction of 5-(hydroxymethyl)furfural

Giancosimo Sanghez de Luna, Phuoc Hoang Ho, Alice Lolli, Francesca Ospitali, Stefania Albonetti, Giuseppe Fornasari, and Patricia Benito*

Dip. di Chimica Industriale “Toso Montanari”

University of Bologna

Viale Risorgimento 4, 40136 Bologna (BO), Italy

E-mail: patricia.benito3@unibo.it

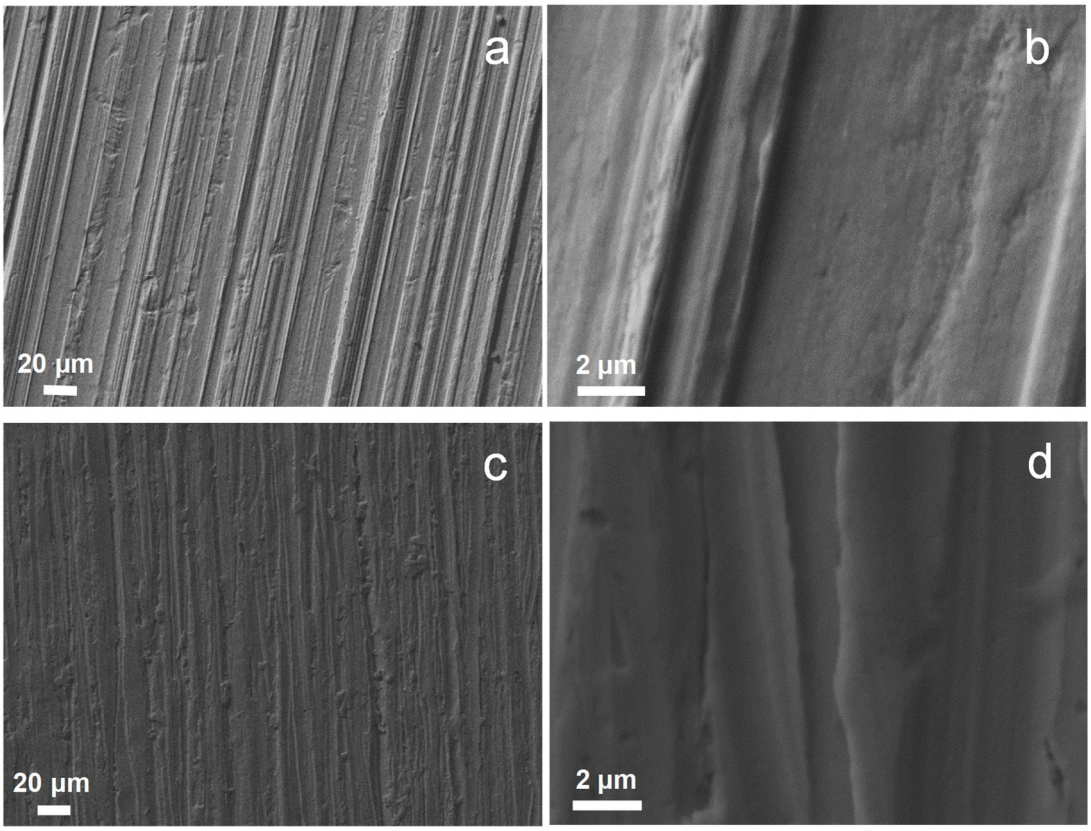

Figure S1. SEM images of Cu (a,b); Ag (c,d) foils.

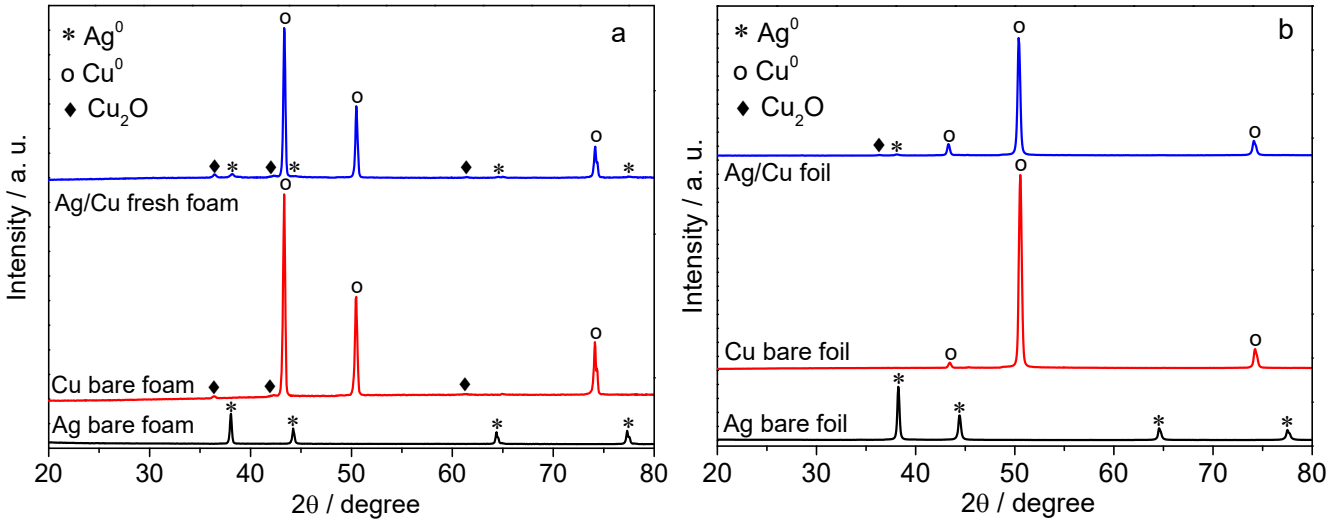

Figure S2. XRD of Ag, Cu and Ag/Cu foams (a) and foils (b) before catalytic tests.

Pb UPD was performed in a single compartment cell with 25 mL of an aqueous solution of 0.10 M sodium potassium tartrate containing 0.01 M H_2SO_4 and 3.10^{-4} M $Pb(NO_3)_2$. The cyclic voltammetries (CV) were measured between 0 and -0.6 V vs SCE at 50 mV/s. The charge corresponding of stripping peak was used for calculation of EASA. The charge calculated for Ag polished (3.10^{-6} C cm^{-2}) was used as reference value.

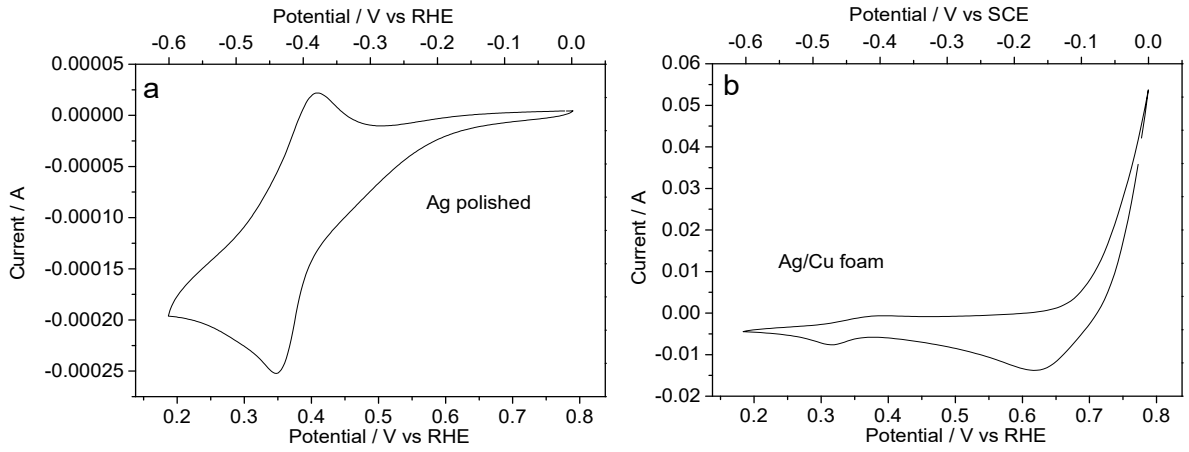

Figure S3. CVs during Pb UPD and stripping on Ag polished foil (a) and Ag/Cu foam (b).

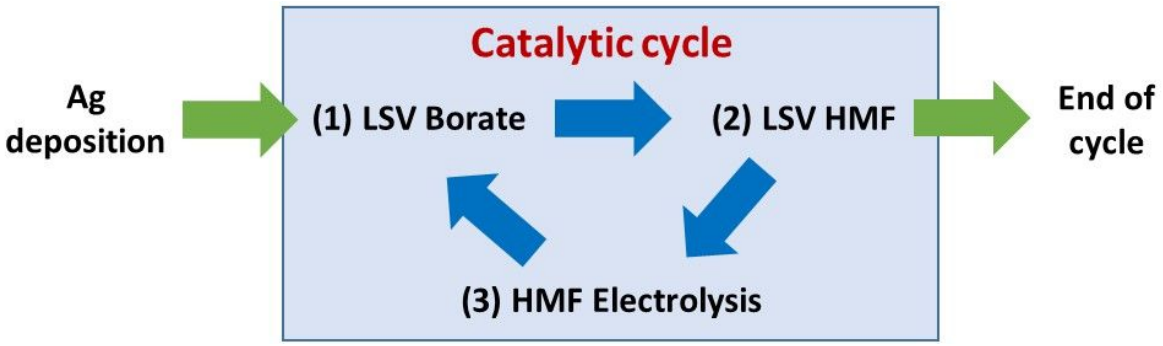

Figure S4. Description of a catalytic cycle. After Ag deposition the catalyst undergoes a LSV in borate buffer (pH= 9.2) and a LSV in borate plus HMF; then HMF electrolysis is performed. The catalytic cycle continues with another LSV in borate and borate plus HMF. Afterwards the cycle can stop or start again keeping constant or modifying the concentration of HMF in the electrolyte.

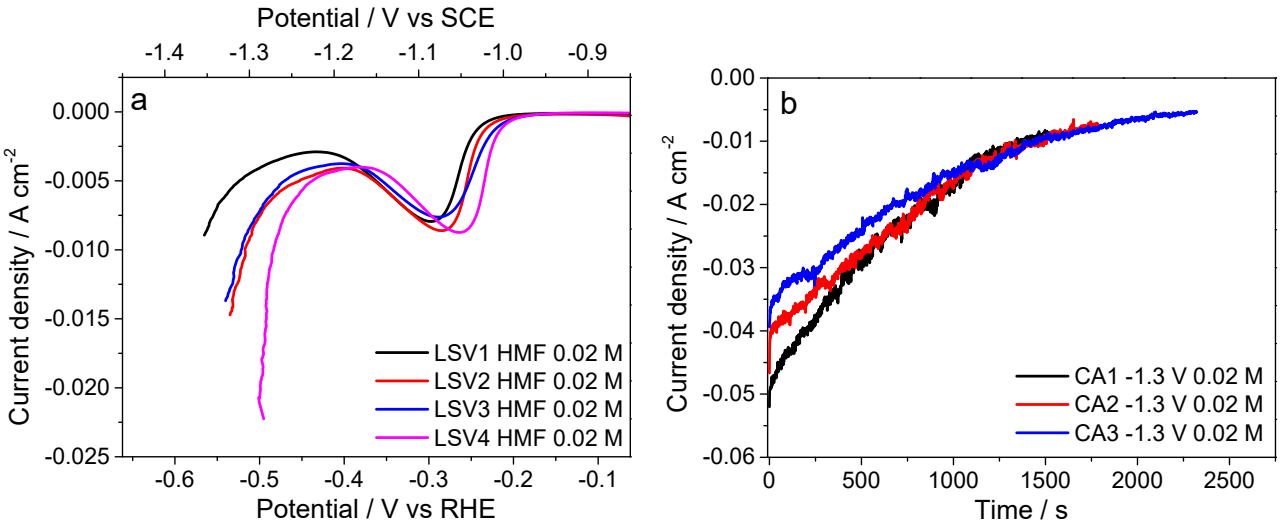

Figure S5. LSVs (a) and current transients during electrolysis (b) over Ag/Cu foam electrocatalyst immersed in 0.02 M HMF electrolytes. The LSVs 1, 2 and 3 were performed just before the respective HMF electrolysis, the LSV4 was performed after the last electrolysis (CA3) and a LSV in borate buffer solution. In (a) LSV range: 0 - -1.4 V vs SCE; scan rate: 5 mVs^{-1} (a). In (b) potential applied: -1.3 V vs SCE (-0.51 V vs RHE).

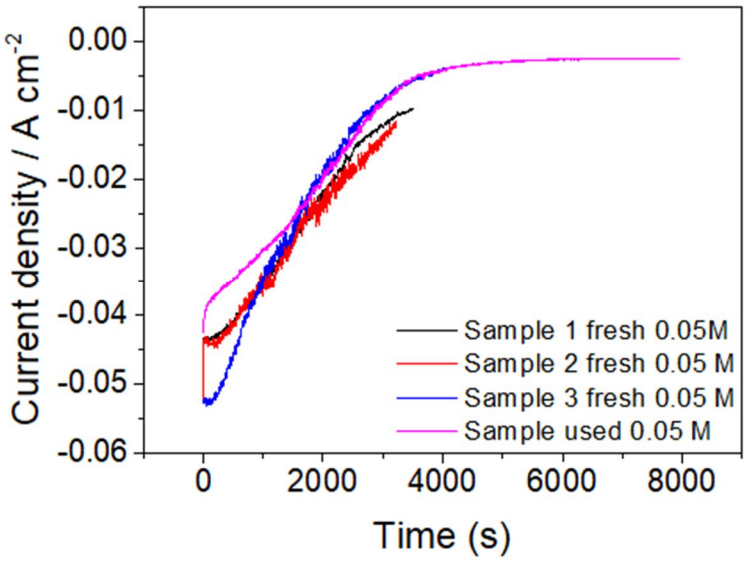

Figure S6. Current transients during electrolysis over different Ag/Cu foams immersed in 0.05 M HMF electrolytes at -1.3 V vs SCE. Comparison between 3 fresh samples and used samples in HMF 0.05 M electrolysis.

Table S1. Results from electrolysis at -1.3 V vs SCE over Ag/Cu samples. Comparison between fresh sample tested only with HMF 0.05 M and Ag/Cu foam already tested using HMF 0.02 M.

Sample	Conv. HMF / %	Sel. BHMF / %	FE. / %	BHMF Productivity / mmol h^{-1} cm^{-2}
Used	100	83	85	0.183
Fresh	97	82	78	0.328

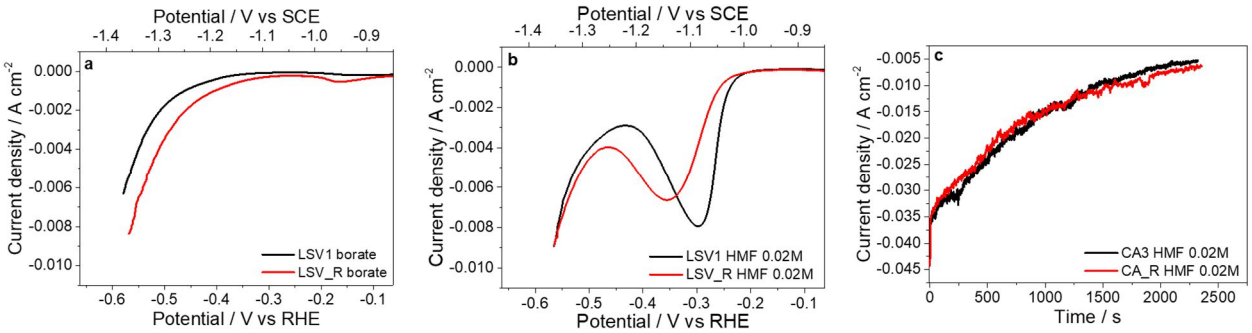

Figure S7. LSVs in borate buffer (pH = 9.2) (a) and 0.02 M HMF in borate buffer (b) over Ag/Cu foam performed before 1st test in HMF 0.02 M and before the "R test". Range: 0 - -1.4 V vs SCE. Scan rate: 1 mV s^{-1} for borate buffer solutions and 5 mV s^{-1} for HMF containing solutions; (c) current transients recorded during the 3rd electrolysis (CA3) and the test 'R' (CA_R) performed in 0.02 M HMF solutions in borate buffer (pH = 9.2) at -1.3 V vs SCE (-0.51 V vs RHE) over Ag/Cu foam.

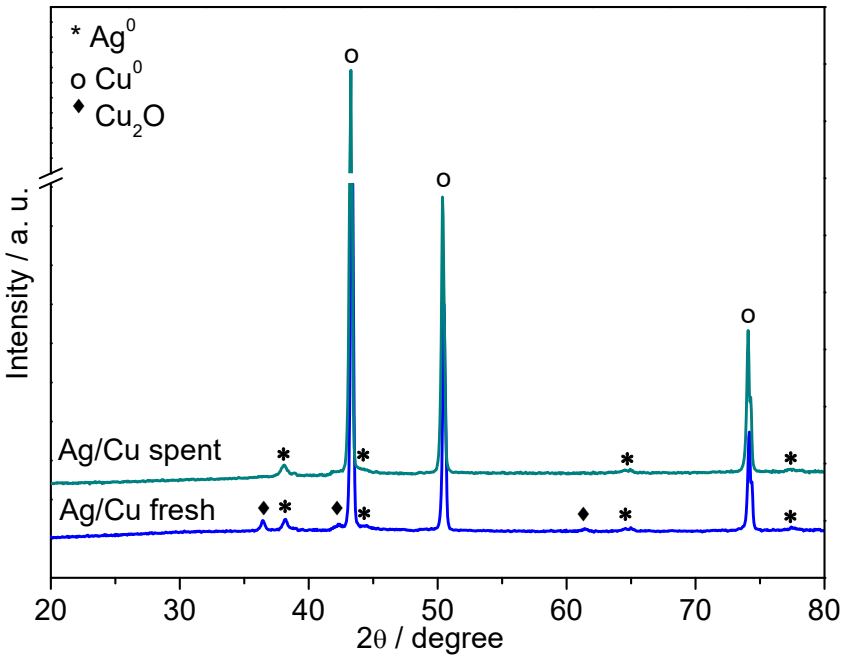

Figure S8. Comparison between Ag/Cu foam catalyst before and after electrocatalytic tests.

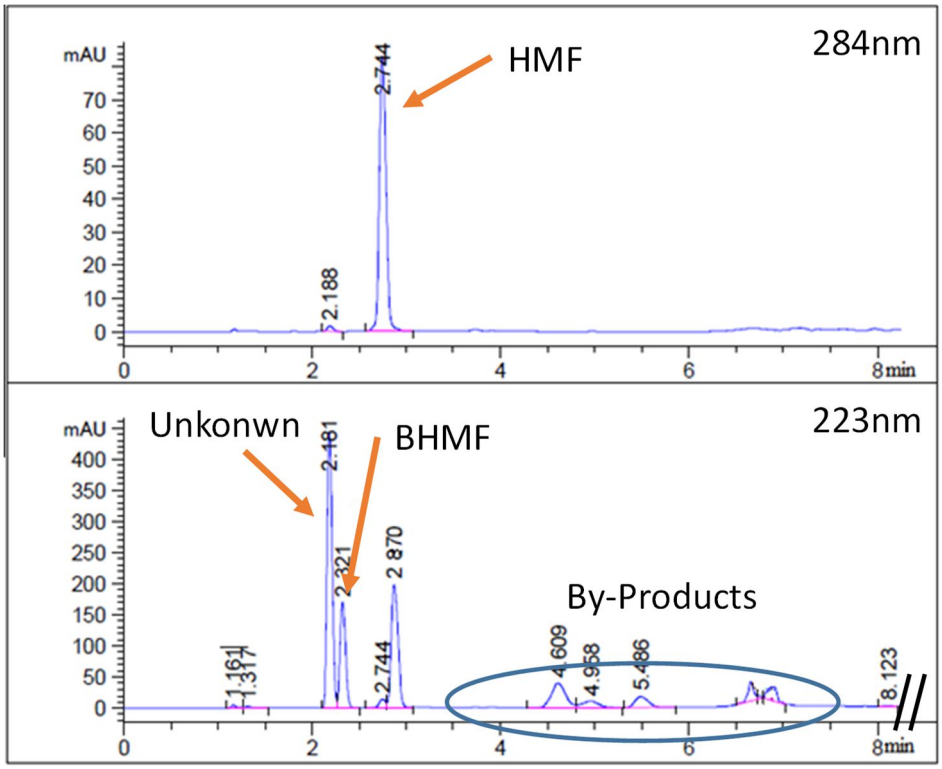

Figure S9. HPLC chromatograms of 0.50 M HMF solution in borate buffer (pH= 9.2) after electrolysis at -1.3 V vs SCE over Ag/Cu foam catalyst. The peak of HMF (Rt = 2.7 min) was identified using a wavelength of 284 nm. The peak of BHMF (Rt = 2.3 min) was identified with a wavelength of 223 nm. The main by-product (Rt = 2.18 min) and the other by-products are visible at 223 nm.

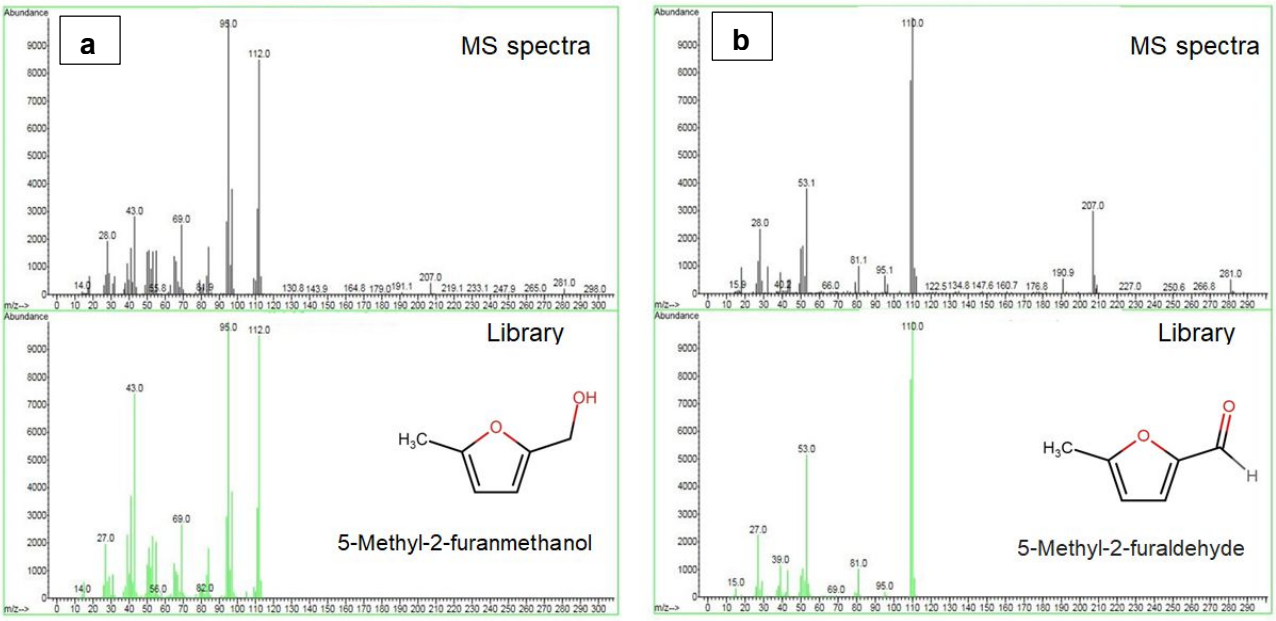

Figure S10. GC-MS spectra recorded in a 0.05 M HMF solution after electrolysis at -1.3 V vs SCE over Ag/Cu foam catalyst and identification of two by-products: 5-methyl-2-furanmethanol (a) and 5-methyl-2-furaldehyde (b).

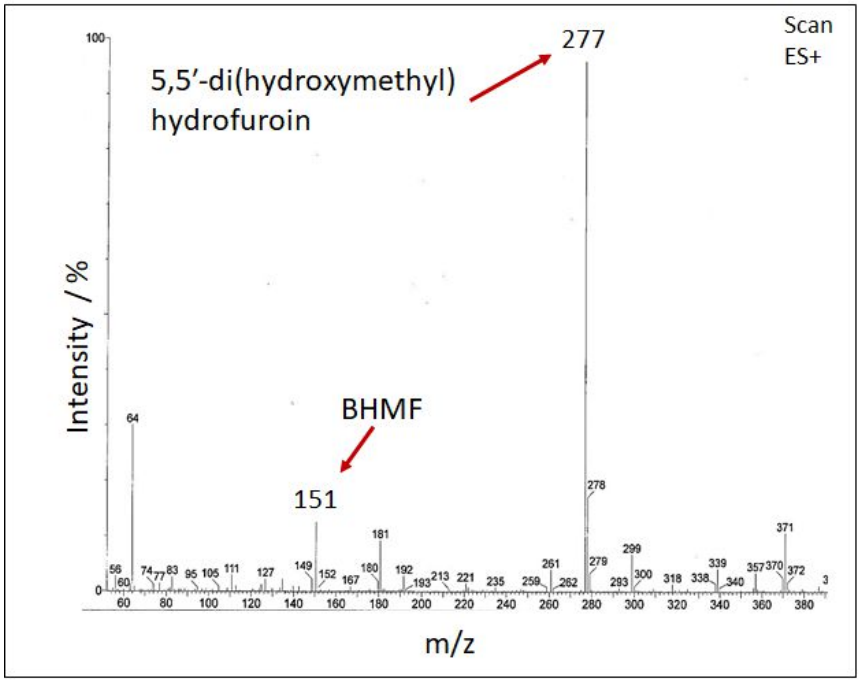

Figure S11. Positive ESI-MS spectra of a 0.05 M HMF solution, after electrolysis at -1.3 V vs SCE, extracted with acetonitrile. In positive scan the peaks give coupling with sodium (m/z 23). The peak with m/z = 151 – 23 = 128 corresponds to BHMF; the main peak with m/z = 277 – 23 = 254 corresponds with the mass of hypothesized hydrofuroin.